Received: 23 May 2016 | Revised: 1 September 2016 | Accepted: 3 September 2016

DOI 10.1002/eco.1792

WILEY

RESEARCH ARTICLE

Evaluating mountain meadow groundwater response to Pinyon-Juniper and temperature in a great basin watershed

Rosemary W.H. Carroll[1] | Justin L. Huntington[1] | Keirith A. Snyder[2] | Richard G. Niswonger[3] | Charles Morton[1] | Tamzen K. Stringham[4]

[1] Desert Research Institute, Reno, NV, USA

[2] US Department of Agriculture-Agricultural Research Service, Great Basin Rangelands Research Unit, Reno, NV, USA

[3] US Geological Survey, Menlo Park, CA, USA

[4] Department of Agriculture, Nutrition and Veterinary Science, University of Nevada, Reno, NV, USA

Correspondence
Rosemary W.H. Carroll, Desert Research Institute, Reno, NV 89512.
Email: rosemary.carroll@dri.edu

Abstract

This research highlights development and application of an integrated hydrologic model (GSFLOW) to a semiarid, snow-dominated watershed in the Great Basin to evaluate Pinyon-Juniper (PJ) and temperature controls on mountain meadow shallow groundwater. The work used Google Earth Engine Landsat satellite and gridded climate archives for model evaluation. Model simulations across three decades indicated that the watershed operates on a threshold response to precipitation (P) >400 mm/y to produce a positive yield (P-ET; 9%) resulting in stream discharge and a rebound in meadow groundwater levels during these wetter years. Observed and simulated meadow groundwater response to large P correlates with above average predicted soil moisture and with a normalized difference vegetation index threshold value >0.3. A return to assumed pre-expansion PJ conditions or an increase in temperature to mid-21st century shifts yielded by only ±1% during the multi-decade simulation period; but changes of approximately ±4% occurred during wet years. Changes in annual yield were largely dampened by the spatial and temporal redistribution of evapotranspiration across the watershed: Yet the influence of this redistribution and vegetation structural controls on snowmelt altered recharge to control water table depth in the meadow. Even a small-scale removal of PJ (0.5 km^2) proximal to the meadow will promote a stable, shallow groundwater system resilient to droughts, while modest increases in temperature will produce a meadow susceptible to declining water levels and a community structure likely to move toward dry and degraded conditions.

KEYWORDS

climate, Great Basin, groundwater dependent ecosystems, integrated hydrologic model, Landsat, Pinyon-Juniper

1 | INTRODUCTION

The increase in abundance and density of woody plants in arid and semiarid ecosystems potentially can have significant ecohydrological implications with respect to water yield and carbon cycling (Huxman et al., 2005). Since the late 1800s, Pinyon-Juniper (PJ) vegetation predominantly composed of single-leaf pinyon (*Pinus monophylla*), and Utah juniper (*Juniperus osteosperma*) have expanded into sagebrush-grasslands throughout the U.S. Great Basin (Miller & Rose, 1999). This has introduced tall-statured, deeply-rooted evergreen species into a community that was formerly short-statured, deciduous, and more reliant on shallow soil moisture. Initiation of PJ expansion could be the result of wetter and milder climatic conditions following the end of the Little Ice Age (Fritts, 1974; Fritts & Wu, 1986), but for many intermountain sites, the timing of PJ expansion is coincident with livestock introduction and fire suppression (Miller & Rose, 1999; Miller, Svejcar, & Rose, 2000; Miller, Bates, Svejcar, Pierson, & Eddleman, 2005). The process of expansion produces an understory with a greatly reduced cover of shrubs and native perennial grasses (Miller et al., 2000). This process results in landscape-scale alterations in habitat

distribution and diversity, biogeochemistry, severe fire potential, and dominance of annual weeds such as cheatgrass (Bromus tectorum L.; Brooks et al., 2004). A decrease in available subsurface water that would otherwise support stream baseflow, springs, and groundwater-dependent ecosystems (GDE; Huxman et al., 2005; Wilcox, Owens, Dugas, Ueckert, & Hart, 2006) also may result. PJ expansion has the potential to change how precipitation (P) is captured and received; the length of time water is needed to maintain plant transpiration; and the magnitude and timing of snowmelt, soil evaporation as well as snow evaporation and sublimation. Woody plant expansion is observed globally (Huxman et al., 2005) contributing to desertification processes by exposing more barren and hydrophobic soil (Madsen et al., 2012) and substantially increasing soil erosion (Grover & Musick, 1990). This expansion should be considered a significant consequence of global change.

PJ removal, or treatment, is a land management option to reduce the negative effects of PJ expansion and restore a functioning and resilient ecosystem containing a more balanced plant community structure resistant to colonization by exotic weed species and re-expansion of PJ (Tausch, Miller, Roundy, & Chambers, 2009). Understanding the sensitivity of water budget shifts in these systems in response to PJ removal is part of maintaining a viable ecosystem. Forested catchments have higher rates of evapotranspiration (ET) than grassy catchments (Zhang, Dawes, & Walker, 2001), and vegetation shifts from woody to non-woody plants should increase water yield (P-ET) through reduction in ET. The interaction between woody plants and surface–subsurface hydrology is complex, however, leading to significant uncertainty about hydrologic response to changing vegetation.

To address this uncertainty, Huxman et al. (2005) outlined a vegetation-streamflow conceptual framework to identify semiarid hydrologic system sensitivity to woody plant expansion based on the notion of woody plants having access to water at depths greater than non-woody plants. Physiographic controls are broadly outlined as riparian versus upland regions. Woody plants in riparian zones have access to shallow groundwater and exert greater control on the hydrologic budget compared to upland areas that have limited access to groundwater. In contrast, plants in upland areas must rely on stored vadose zone soil water to supply water for transpiration needs. Niche partitioning in these upland, water-limited environments has traditionally relied on a two-layer conceptual model in which plant morphology dictates use of stored water with herbaceous plants relying on shallow soil water and woody plants relying on deeper soil water (Walter, 1971). More recently, ideas on plant water resource partitioning have shifted to emphasize the function of shallow and deep pools of water (Ryel, Ivans, Peek, & Leffler, 2008; Ryel, Leffler, Ivans, Peek, & Caldwell, 2010). Shallow soil water is proposed as a highly competitive "growth pool." During periods favorable for plant growth that require high-resource acquisition, all plant species will compete for water and nutrients from this shallow soil zone. When this shallow pool of water diminishes and water becomes limited, plants either senesce (annual and perennial grass and forb species) or maintain physiological function by relying on deeper stored water during the summer dry periods and drought. In support of this concept, Mollnau, Newton, and Stringham (2014) found that PJ successfully competes with grasses and forbs for shallow soil water (<30 cm) but is likely the dominant and perhaps only influence responsible for depleted water reserves at greater depths (>200 cm).

Thin soils are typical in the upland reaches of Great Basin watersheds, and there is limited potential for soil water storage. However, growing evidence suggests that weathered and fractured bedrock in upland regions may be hydrologically active and can play an important role in sustaining transpiration in seasonally water-limited environments (Schwinning, 2010; Salve, Rempe, & Dietrich, 2012; Huntington & Niswonger, 2012).

Conceptually, removal of PJ from upland reaches in a watershed may have the potential to reallocate water toward lateral (interflow) and vertical (recharge) subsurface flow. Uncertainty in hydrologic response to changes in vegetation is compounded by the scale dependence of ET components in both space and time with changes in yield generally declining as analysis increases in scope from the tree to stand to watershed scale (Wilcox et al., 2006). While extensive work has focused on hydrologic repartitioning as a consequence of watershed-scale forest disturbance related to pests (Biederman et al., 2014; Bearup, Maxwell, Clow, & McCray, 2014; Mikkelson et al., 2013; Pugh & Gordon, 2013), fire (Seibert, McDonnell, & Woodsmith, 2010), and woodland management (Robles et al., 2014), no study (to the authors' knowledge) has focused on the influence of PJ on watershed-scale water budgets and GDEs in the arid and semiarid landscape of the Great Basin.

GDEs, such as mountain meadows, are zones of groundwater discharge primarily through phreatophyte ET and are important in that they support much of the ecological biodiversity in the Great Basin. In addition to a lack of understanding of how Great Basin GDEs respond hydrologically to upland PJ, little is known about how these systems will respond to climate shifts in the region. Climate in the Great Basin already has experienced warming trends during the last century of 0.3°C to nearly 1.0°C, and a decline in winter snowpack has been observed (Wagner, 2003; Mote, Hamlet, Clark, & Lettenmaier, 2005; NOAA 2016). Warming trends are expected to continue into the future. A multi-model aggregation of global climate models using output from the Coupled Model Intercomparison Project, Phase 5 estimates mean annual temperature increases in central and eastern Nevada for the mid-21st century (2041–2070) of 2.5°C to 3.5°C over historical conditions (1950–2005) for reactive carbon pathway (RCP) 4.5 and 8.5, respectively. Historical conditions from 1895 to 2015 (NOAA, 2016) indicate P increases from 1969 to 1986 after which drying has subsequently negated any definitive trend in P since the mid-20th century. Global climate models likewise suggest neither significant nor robust change in P by the mid-21st century (Abatzoglou et al., 2014). Increased levels in CO_2 and modest increases in temperature will favor C3 photosynthetic pathways through increased production and water use efficiency to benefit both native grasses and invasion of cheatgrass (Ziska, Reeves, & Blank, 2005), and it is anticipated that perennial forbs and woody species also could be at an advantage (Chambers, 2008). Rising temperatures will alter P type (rain vs. snow) and influence potential ET (PET), but it is unknown to what degree these changes will affect GDE shallow groundwater reserves and their ability to sustain viable ecologic biodiversity.

2 | OBJECTIVE

The objective of this study was to (a) better understand the magnitude and timing of water budget shifts based on PJ distribution and

mid-21st century climate projections for a snow-dominated, semiarid watershed located in central Nevada, and (b) explore how shallow groundwater in a mountain meadow will respond to these changes through use of field observations, satellite remote sensing of meadow vegetation vigor, as well as integrated surface and groundwater modeling of the watershed. The study area is representative of rangelands of the Intermountain West in the U.S. where PJ is estimated to have expanded (and infilled) into 18 million hectares, of which 66% is estimated to have been treeless prior to the 1860s (Miller, Tausch, McArthur, Johnson, & Sanderson, 2008). Water budget shifts associated with PJ expansion and rising temperature are likely to change the hydrologic partitioning of shallow soil moisture, interflow, and groundwater recharge, altering ET consumption of down-gradient phreatophyte vegetation. The approach presented here allows for robust analysis and consideration of complex surface and groundwater interactions, feedbacks, and timing of important water states and fluxes.

3 | SITE DESCRIPTION

The 11 km^2 Porter Canyon Experimental Watershed (PCEW) is located in the Desatoya Mountain Range in central Nevada (Figure 1). Elevation in the watershed ranges from 2032 to 2637 m with mean annual P directly correlated to elevation. Estimated mean annual P is 360 ± 98 mm/y with the majority of P falling as snow during winter months. Average monthly minimum and maximum temperature for the period of record (1981–2013) ranges from −11.5°C in January to 27.8°C in August. Geology within the watershed is composed of early Oligocene to early Miocene rhyolite in the upland mountain block, with alluvial material in the valley bottom and stream corridor. A steep-walled, fault-controlled bedrock canyon defines the outlet of the watershed and is the apex of a large alluvial fan below. PJ occupies nearly 80% of the watershed area, with canopy densities ranging from 10% to 60%. Northern aspects contain lower density stands of PJ, more mountain sagebrush, and the only occurrence of snowberry (*Symphoricarpus sp.*). Great Basin Xeric mixed shrub is the second largest vegetation type and occurs primarily in the upper watershed at elevations higher than 2400 m (LANDFIRE, 2008). Keystone plant species are used to characterize dry, mesic, and wet meadow conditions and are associated with five 30 m transects and depth to water (DTW) in shallow groundwater piezometers (Figure 2). The obligate phreatophyte, Nebraska Sedge (*Carex nebrascensis*), occurs within the wet meadow zones, while facultative phreatophytes of Douglas Sedge (*Carex douglasii*) and Field Sedge (*Carex praegracilis*) occur in the mesic plant community. The dry meadow contains mostly Mountain Big Sage (*Artemisia tridentate vaseyana*) and Western Wheatgrass (*Pascopyrum smithii*). Wet and mesic vegetative complexes have observed DTW ranging from 0.5 to 2 m, respectively, and are fairly stable at seasonal and annual timescales. Observed DTW in dry and degraded upland

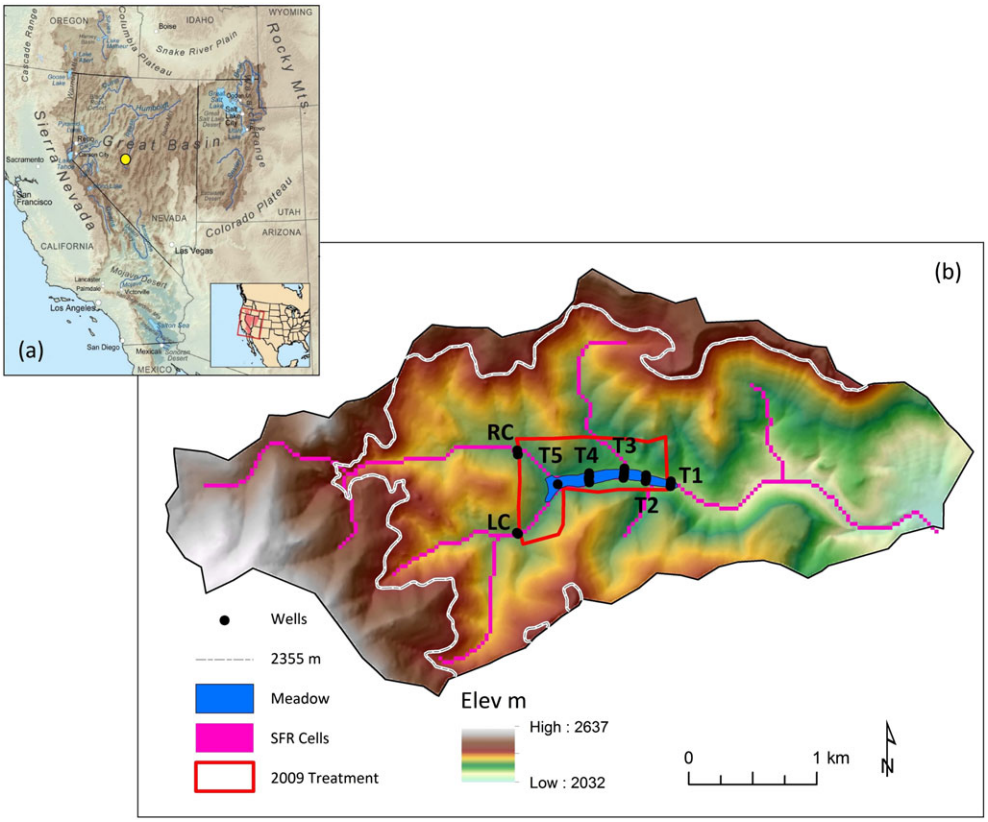

FIGURE 1 Location of the (a) Great Basin within the intermountain western U.S. (modified from https://greatbasinseeds.com) with Nevada (NV) delineated and the study site identified in central NV; and (b) Porter Canyon Experimental Watershed shown in a color coded digital elevation map. Identified are the groundwater piezometer clusters installed in 2009 with IDs in order of decreasing gradient (RC, LC, T5-T1). The mountain meadow area is shaded in blue, while the area of the 2009 PJ treatment (small-scale) is delineated with a red polygon. Also shown are stream flow routing (SFR) package model stream cells and the elevation of 2355 m below which pre-expansion PJ is assumed not to exist

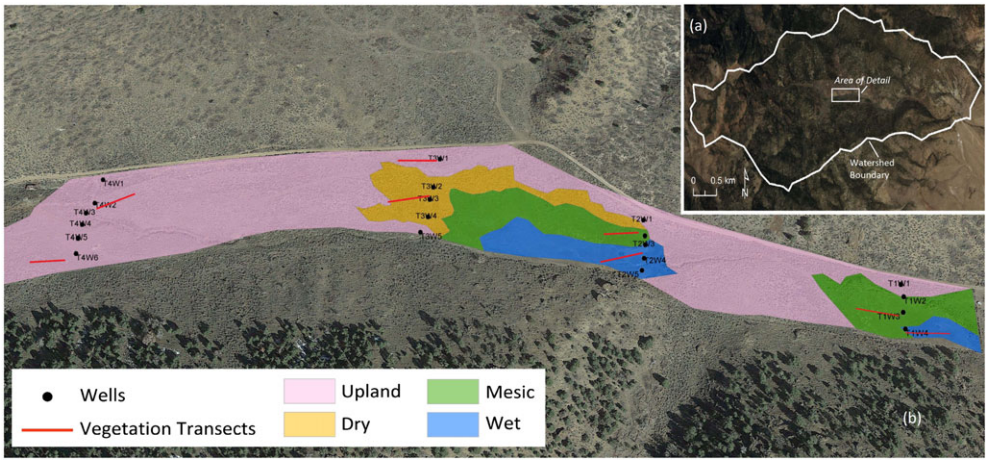

FIGURE 2 Image of (a) the Porter Canyon Experimental Watershed, and (b) a detail of the mountain meadow study area with vegetation zones, transects, and groundwater piezometers (wells) identified. Google Earth image acquired from March 22, 2014

communities is generally greater than 5 m, with rapid fluctuations during wet and dry periods.

Stream discharge exits the PCEW only during pluvial events, such as witnessed in 2011 (P = 537 mm/y) but otherwise has not been observed with flow. Anecdotal evidence suggests that the stream may have flowed more regularly, given that a 79 mm/y (2420 m^3/d) surface water right is decreed near the outlet of the watershed. In the early 1900s, a small reservoir and substantial irrigation infrastructure channeled water approximately 8.5 km^2 out of the lower canyon and into the valley flats. It is unknown if PJ expansion is linked to the possible loss of surface water. In 2009, PJ treatment consisted of felling trees perpendicular to the slope and removing limbs on the underside of the bole to facilitate contact with the ground. This approach minimized erosion and was conducted on 0.5 km^2 (140 acres) in the vicinity of the meadow area (Figure 1). Plans are in place to expand treatment by an additional 9.3 km^2 (2300 acres) in the future. Following the initial PJ treatment in the spring of 2009, 24 shallow groundwater piezometers, a soil climate analysis network (SCAN) station, and four stream flow weirs were installed in the meadow. At this time, plot-scale research on vegetation type and distribution, along with spring flow measurements, was initiated.

4 | APPROACH

Our general approach for evaluating potential changes to water budget components and meadow groundwater conditions due to PJ expansion and mid-21st century changes in climate relied on scenario testing using an integrated surface and groundwater model (groundwater and surface water flow [GSFLOW]), and comparing and contrasting simulated hydrologic states and fluxes for different scenarios related to PJ distribution and climate.

5 | METHODS

5.1 | Integrated surface and groundwater modeling

GSFLOW (Markstrom, Niswonger, Regan, Prudic, & Barlow, 2008) combines the U.S. Geological Survey (USGS) precipitation-runoff modeling system (PRMS; Leavesley, Markstrom, Viger, & Hay, 2005) with the USGS modular groundwater flow model (Harbaugh, 2005; Niswonger, Panday, & Ibaraki, 2011) to account for flow within and between the plant canopy and soil zone, streams, and shallow groundwater system. GSFLOW has been used for a variety of studies in the Great Basin related to changing climate and potential impacts to GDEs and groundwater resources (Huntington & Niswonger, 2012; Huntington et al., 2013; Rajagopal et al., 2015; Tang, Carroll, Lutz, & Sun, 2016). The model grid resolution is 30 m, with four layers representing shallow alluvium and mountain block rhyolite units. Maximum depth of alluvium is assumed to be 15 m along valley axis, tapering to 1 m at margins and is modeled with two layers of equal thickness. Rhyolite is also modeled as two layers. The upper rhyolite layer is assumed to be 15 m thick, weathered and fractured, and more permeable than the lower rhyolite layer. The lower layer is assumed to be 60 m thick and represents intact rhyolite that has low permeability. Groundwater discharge likely occurs through the alluvium and fractured rhyolite onto the alluvial fan at the exit of the canyon. This is simulated as a general head boundary (GHB; Harbaugh, 2005) condition in which the saturated thickness within the alluvium is held at approximately 5 m. Porter Creek was simulated using the streamflow-routing (SFR) package (Niswonger & Prudic, 2005) and Manning's wide-channel assumption with width scaled from 0.3 to 3 m based on digital elevation map calculated accumulated flow.

Vegetation was delineated using the USGS LANDFIRE raster data set designating vegetation type and density at 30 m grid resolution. Vegetation information was used to derive PRMS parameters of dominant cover type, summer and winter cover density, canopy interception characteristics for snow and rain, and transmission coefficients for shortwave radiation. Table 1 defines post-treatment vegetation assemblages at the sub-GSFLOW grid resolution for the alluvial and hillslope regions of PCEW. Replacement vegetation fractions were defined using observed vegetation along 30 m transects after 6 years following the 2009 PJ removal with slight modification along hillslopes to incorporate the ideal of 20% cover by perennial native herbaceous species (both grasses and forbs) to prevent significant increases in cheatgrass identified to occur in similar warmer and drier sites (Chambers et al., 2014). PRMS post-treatment 30 m grid-scale

TABLE 1 Ratios of post-treatment replacement vegetation observed along transects in Porter Canyon Experimental Watershed. Hillslope ratios rescaled after including the ideal fraction of grasses to promote resistance to annual invasive species

Type	Alluvium	Hillslope
Bare	0.27	0.40
Grass	0.57	0.20
Shrub	0.16	0.40
Pinyon-Juniper	0.00	0.00

vegetation parameters were calculated as an area-weighted average based on these fractions (Table 2). Replacement vegetation effectively reduces cover density by 5%, winter P interception capacity by 5–25%, and summer P interception capacity by 3–5%, while increasing the transmission of shortwave solar radiation during winter months by 12 to14% compared to PJ characteristics prior to treatment.

Climate inputs of daily minimum and maximum temperature and P for water years 1981–2013 were derived through a combination of the on-site SCAN station located within the meadow (elev. = 2194 m; record = 2009–2013) and Parameter-elevation Regression on Independent Slopes Model mean monthly P patterns across the watershed (Daly, Neilson, & Phillips, 1994; PRISM Climate Group, 2015). The period of record of the SCAN site was extended using the Big Creek SNOTEL site (elev. = 2650 m) located approximately 50 km to the east on the western slope of the Toyiabe Mountains through monthly correlations between stations during overlapping periods of data collection. Daily climate data drive GSFLOW calculations to spatially distribute P, solar radiation, evaporation, transpiration, sublimation, snowmelt, surface runoff, and infiltration across the watershed (Markstrom et al., 2008). GSFLOW's repeat option (Regan, Niswonger, Markstrom, & Barlow, 2015) was used to stitch together a 10-year spin-up, followed by a pre-2009 treatment (1981–2009) and post-2009 treatment (2009–2013) to allow for change in vegetation type and distribution in the region of PJ removal (Figure 1). Changes in model vegetation parameters were applied only to those model cells designated as PJ prior to treatment. The 10-year spin-up was determined to be adequate based on ability of soil as well as unsaturated and groundwater storage to reach quasi-equilibrium for given climate forcing. The importance of this was to remove the influence of estimated initial hydrologic state on the solution of fluxes. Figure 3 illustrates the GSFLOW simulation strategy with calibration limited to the historical period of 2009–2013 based on available observed data. Iterations were required to converge on a solution with spin-up output representative of the chosen suite of model input parameters. Calibration was accomplished by adjusting PRMS and MODFLOW parameters to best match observed SCAN shortwave solar radiation and reference ET (ET_o) in which ET_o was calculated with the ASCE standard Penmen Monteith equation estimates for a grass surface. The calculation incorporates solar radiation, temperature, humidity, and wind speed (ASCE-EWRI, 2005). Calibration also was done to match observed groundwater levels in meadow piezometers collected from 2009 to 2013 and by replicating observed stream flow in 2011, but otherwise simulating a lack of observed streamflow.

5.2 | Remote sensing of meadow vegetation

The normalized difference vegetation index (NDVI) corresponds to the relative density and vigor of vegetation through absorption and reflectance of red and near-infrared wavelengths of the electromagnetic spectrum (Tucker, 1979). Optical vegetation indices such as NDVI are commonly used in the Great Basin to estimate ET (Nichols, 2000; Devitt et al., 2011; Beamer, Huntington, Morton, & Pohll, 2013), plant cover (Nichols, 2000), phreatophyte areas (Smith, Laczniak, Moreo, & Welborn, 2007), leaf xylem water potential (Baghzouz, Devitt, Fenstermaker, & Young, 2010), shallow groundwater levels (Carroll, Pohll, Morton, & Huntington, 2015), and GDE conditions (Huntington et al., 2016). Following the processing workflow of Huntington et al. (2016), we used Google's Earth Engine (EE) cloud computing and environmental monitoring platform (Moore & Hansen, 2011) to access and process Landsat 5 thematic mapper and Landsat enhanced thematic mapper archives from 1984 to 2013 to compute spatially averaged August mean NDVI for the mountain meadow area. NDVI was chosen instead of other optical vegetation indices or combined optical-thermal

TABLE 2 Comparison of PRMS vegetation parameters for pre- and post-treatment

PRMS parameter	Description[a]	Units[b]	Pre-treatment[c]	Post-treatment[d]	
				Alluvium	Hillslope
cov_type	Principal vegetation (0 = bare; 1 = grass; 2 = shrub; 3 = deciduous; 4 = conifer	NA	4	1	2
covden_sum	Summer vegetation density for major vegetation type	Fraction	0.31 ± 0.07	0.27	0.27
cov_den_win	Winter vegetation density	Fraction	0.31 ± 0.07	0.21	0.19
snow_intcp	Snow interception storage capacity	cm	0.25 ± 0.00	0.00	0.03
srain_intcp	Summer rain interception storage capacity	cm	0.13 ± 0.0	0.10	0.08
wrain_intcp	Winter rain interception storage	cm	0.13 ± 0.03	0.03	0.08
rad_trncf	Transmission coefficient for short-waver radiation through winter vegetation canopy	Fraction	0.44 ± 0.09	0.56	0.58

PRMS = precipitation-runoff modeling system; PJ = Pinyon-Juniper.

[a]Applies to major vegetation type in modeled cell.

[b]PRMS input units of length are inches but converted to SI for table.

[c]Mean ± SD for PJ cells.

[d]Applied only to cells designated PJ prior to treatment.

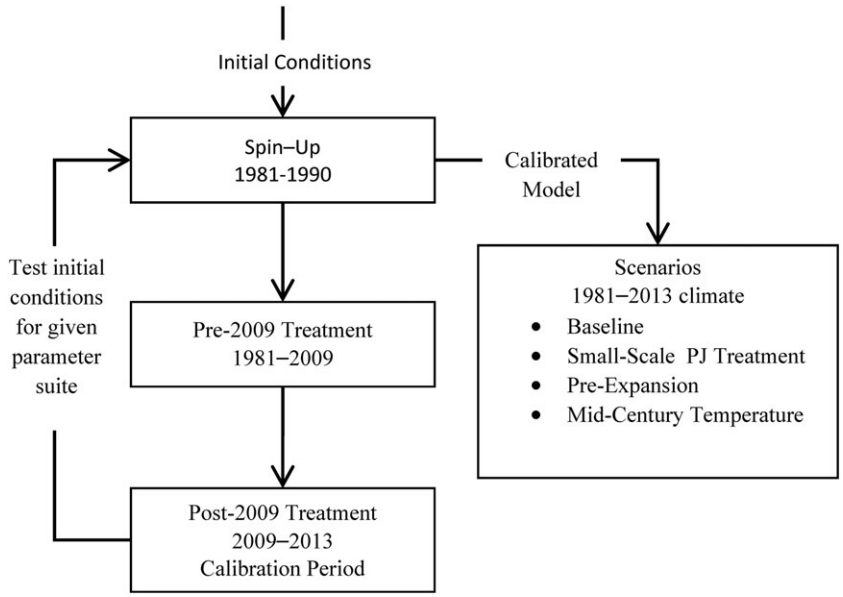

FIGURE 3 Groundwater and surface-water flow simulation strategy. Scenarios are defined in the Section 5.3

indices (Qi, Chehbouni, Huete, Kerr, & Sorooshian, 1994; Mallick, Bhattacharya, & Patel, 2009) since NDVI has been shown to better estimate sparse-to-moderate vegetation cover in arid environments (McGwire, Minor, & Fenstermaker, 1999; Wu 2014), has a long history of usage, and does not require parameter calibration. Landsat scenes acquired during August were selected to limit the NDVI signal of shallow-rooted grasses and forbs as well as to maximize the phreatophyte NDVI signal derived from deeper soil moisture and groundwater. North American Land Data Assimilation System (Mitchell et al., 2004) hourly temperature and humidity were used within the EE framework for Landsat atmospheric correction and at-surface reflectance computations following Tasumi, Allen, and Trezza (2008). We then compared annual NDVI time series to GSFLOW simulated average soil moisture and DTW within the meadow areas as independent evaluation of integrated modeling results during the simulated historical period.

5.3 | Sensitivity to changes in PJ and temperature

Using the calibrated hydrologic model, we ran four scenarios to test sensitivity of water budget components and mountain meadow groundwater level response to changes in PJ and mid-21st century temperature for central Nevada. All scenarios include the 10-year spin-up developed during calibration.

1. *Baseline* conditions represent pre-2009 PJ treatment distribution and use historical climate from 1981 to 2013. No change to PJ distribution was simulated. All other scenarios were compared to baseline to assess system response.
2. *Small-Scale* PJ treatment simulates removal of PJ from 0.5 km^2 in the vicinity of the mountain meadow (Figure 1) for the entire simulated period with climate forcing equal to baseline. Model cells within the treated area that contain PJ were converted to PRMS vegetation parameters provided in Table 2 of replacement vegetation. Results were investigated to establish if small-scale removal of PJ could impact meadow groundwater response or if removal at this scale would not be sufficient to produce change.
3. *Pre-Expansion* assumes that PJ occupied 20% of the basin by area prior to its expansion during the 20th century. A cumulative distribution of PJ as a function of basin area and elevation found maintaining PJ at elevations above 2355 m established PJ at 20% by area. PJ occupying area below 2355 m was assigned PRMS vegetation parameters provided in Table 2. Climate forcings were equal to baseline. The total area converted from PJ to post-treatment conditions was approximately 7.7 km^2 (1900 acres) and represented a realistic management option while also allowing a test of hydrologic response to conditions prior to PJ expansion into the downslope region of sagebrush-grassland complexes.
4. *Mid-Century* temperature change was applied to the baseline condition as a uniform 3.0°C increase to minimum and maximum daily temperature throughout the simulation. This represented a mean estimated annual temperature increase based on RCP4.5 and RCP8.5. No change in P was simulated due to lack of consensus or robustness in estimated change by mid-21st century. Change in P type (rain or snow) was allowed to vary based on air temperature. The approach was simplistic, but provided insight into hydrologic thresholds based on predicted changes in climate for central Nevada at the intermediate timescale.

6 | RESULTS

6.1 | Model calibration

Calibration of GSFLOW was done in a three-step process. First, multi-year, monthly climatologies of shortwave solar radiation and ET_o were calibrated by adjusting respective PRMS parameters until simulated values closely matched observed climatologies derived at the SCAN site from October, 2009, to December, 2013. Daily comparisons of

simulated and observed ET_o are provided in Figure 4, with predicted variability capturing the range in daily observations. Second, groundwater conditions were modeled as unconfined with MODFLOW parameters of specific storage assumed 1e-6, while hydraulic conductivity of all layers was assumed to be isotropic. Hydraulic conductivity of the alluvium (layers 1 and 2) and deeper rhyolite (layer 4) were defined as 1 and 0.001 m/d with specific yield assigned as 0.10 and 0.005, respectively, based on representative units in the Great Basin (Belcher, Elliot, & Geldon, 2001; Welch, Bright, & Knochenmus, 2007). Predicted water levels were found to be insensitive to the conductance of the GHB defining groundwater flux out of the basin onto the alluvial fan. Therefore, conductance was increased such that the GHB represented a constant head condition. Observed water levels were best matched by adjusting hydraulic conductivity and specific yield of the shallow, fractured rhyolite (layer 3). These were adjusted to 0.1 m/d and 0.01, respectively, to minimize error in prediction. Calibrated hydraulic conductivity values fell between the values defining transmissive alluvial units and the less permeable, intact rhyolite unit; were consistent with the conceptual model and at the upper range for volcanic flow units in the region (Belcher et al., 2001). PJ were assumed to access deeper saturated water and able to use water from the unsaturated zone at low water content. A regression of monthly simulated versus observed water level elevations is provided (Figure 5) with a root-mean squared error equal to 1.8 m, or 2.8% across the range of observed water levels. Figure 6 compares monthly DTW for wells spanning different vegetation zones (Figure 2). Simulated temporal response in wells replicated observed behavior despite the 30 m grid scale of GSFLOW and use of a single set of hydraulic parameter values for individual hydrostratigraphic units. Observed DTW in the up-gradient well (RC2; degraded meadow) trended toward drying every year, with DTW approaching the bottom of the well. Spring rebound in water levels was rapid, while dry years showed continuous periods of deeper DTW and less spring rebound. Simulated response missed some of the annual variability but captured the maximum observed rebound in 2011, and the deeper DTW trend experienced afterward. Mid-gradient wells (T4W4; degraded meadow and T3W3; dry meadow) did not experience annual drying and were observed with fairly consistent DTW through time (3–4 m). The exception was 2011 with a large response in water levels to above average P. Modeled results captured the quasi-steady state water levels prior to 2011 and the maximum rebound in 2011 with water levels reaching land surface, but simulated results tended to over emphasize water level response during subsequent drier years. The representative down-gradient well (T2W2; mesic meadow) was observed with water levels hovering around 1 m below land surface, drawdown toward 2 m during dry years, and water levels reaching land surface in 2011. Simulated response was similar, although the model over predicted drawdown slightly.

The third calibration step was to match the singularly observed flow event in 2011 (0.028 m^3/s or 79 mm/y). This was accomplished by adjusting the PRMS maximum soil storage parameter (*SSP*; cm), conceptualized as a field capacity threshold above which water is partitioned as either lateral interflow through the soil zone or percolating downward as gravity drainage into the unsaturated zone. The spatial distribution of *SSP* was first estimated as the product of rooting depth and available water content. Rooting depth was estimated by reclassifying LANDFIRE 30 m raster with ranges spanning 0 cm for bare ground, 46 cm for grasses and biennial forbs, 61 cm for Sagebrush Steppe, and 76 cm for Sagebrush Shrubland and PJ woodlands. Available water content was extracted from the soils survey geographic database data set (NV768 and NV770; Natural Resources Conservation Service, 1991) to establish 10 m raster cells and then aggregated to the 30 m GSFLOW grid by taking the mean. Satisfactory calibration was accomplished by maintaining the spatial distribution of *SSP* and scaling uniformly by a factor of 1.45 across the basin. An increase in *SSP* allowed for more water to be stored in the soil zone and available for losses related to evaporation and transpiration and thereby decreased water movement through runoff, interflow, or recharge.

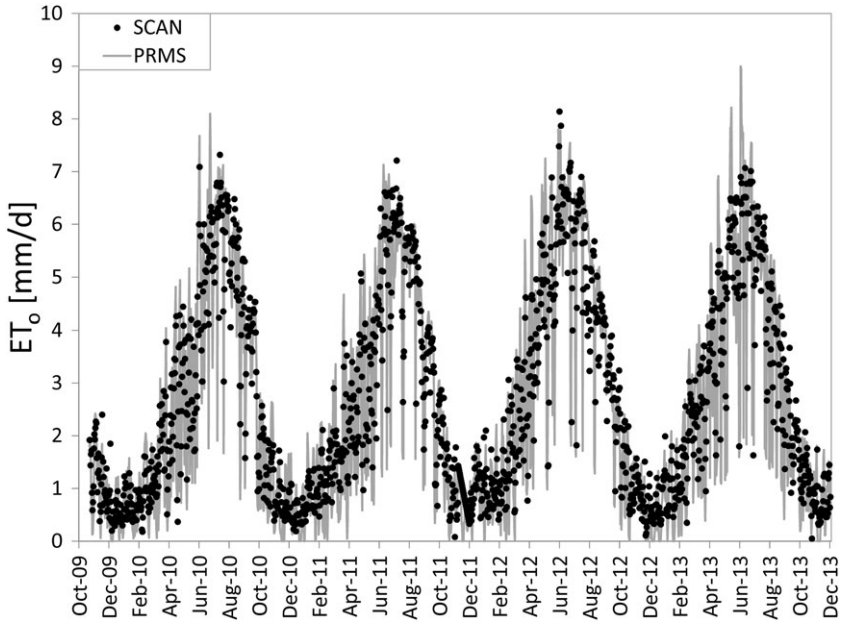

FIGURE 4 Comparison of precipitation-runoff modeling system (PRMS) simulated and computed reference ET (ET_o) using soil climate analysis network (SCAN) station data of solar radiation, temperature, humidity, and wind speed. ET_o was computed using the ASCE standard Penmen Monteith equation for a grass reference surface (ASCE-EWRI, 2005)

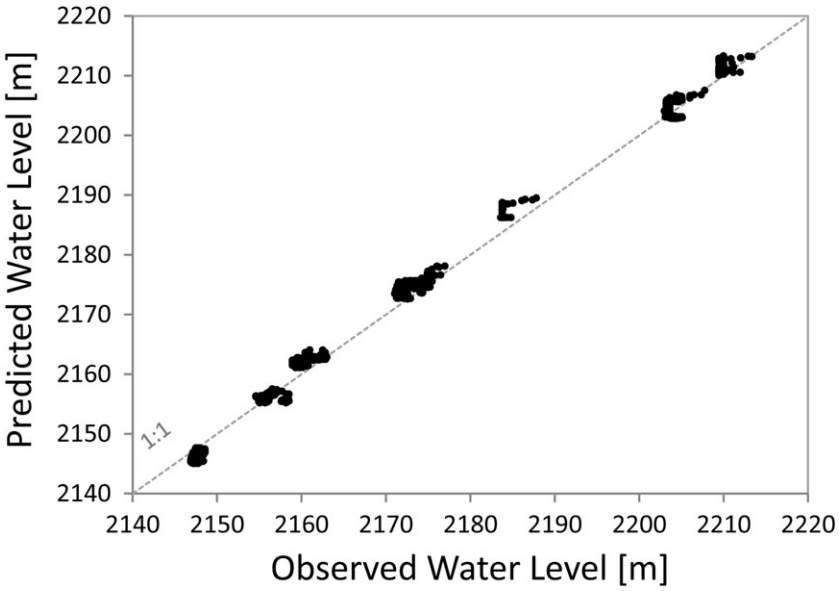

FIGURE 5 A comparison of observed and predicted mean monthly water levels

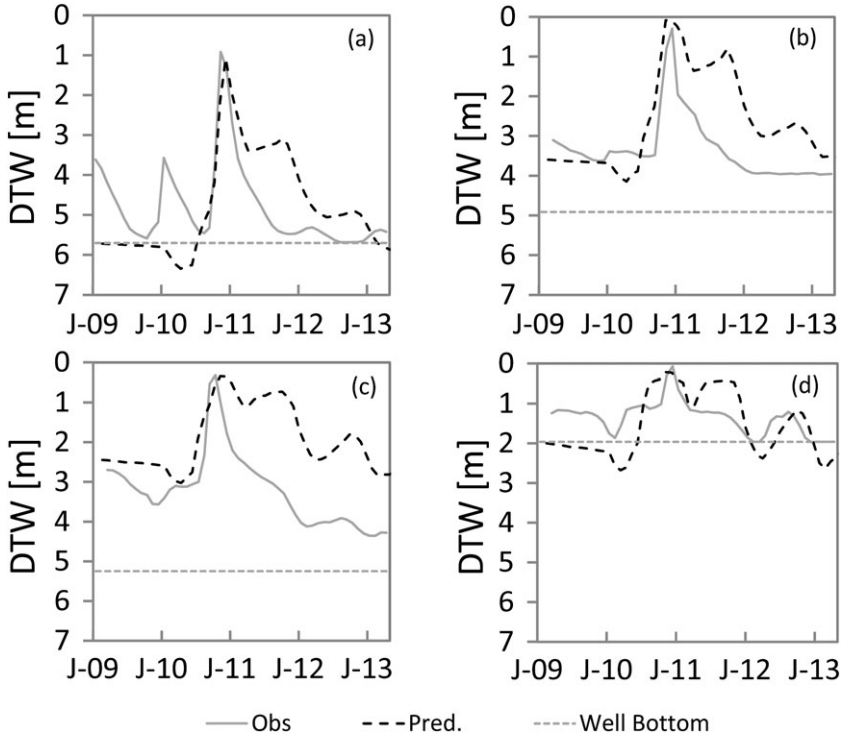

FIGURE 6 Comparison of predicted (dashed black line) to observed (solid gray line) monthly depth to water (DTW): January (J) 2009 through December 2013 for (a) RC2, degraded meadow; (b) T4W4, degraded meadow; (c) T3W3, dry meadow; and (d) T2W2, mesic meadow. Well bottom is illustrated as a dashed gray line. Locations of wells are provided in Figures 1 and 2

6.2 | Baseline water budget

From 1981 to 2013, mean annual P in the basin was 363 mm/y, with simulated snow water equivalent (SWE) equaling 72% of P. The baseline scenario produced an average yield of −0.23%, indicating the basin functions near equilibrium (ET = P) at the multi-decadal scale. Simulated ET losses were divided into soil evaporation and plant transpiration (78%), snow evaporation (11%), and canopy evaporation (5%) as well as groundwater ET (6%) and groundwater discharge to the alluvial fan (0.2%). Several annual water budget components are presented in Figure 7 with P ranging from 237 (2000) to 588 mm/y (1983) and SWE from 53% (2013) to 83% (2008) of P. Results indicated a threshold hydrologic response to $P > 400$ mm/y with these wet years producing a positive yield, or P > ET. During wet years, P was sufficiently large to promote recharge, increase groundwater storage, and generate streamflow. With increased recharge and groundwater storage, DTW decreased (Figure 8) and increased groundwater ET occurred to mitigate some of the positive yield response in the system. The exception to this threshold response to P was 1982 in which more than 124 mm of snow fell at the very end of September. This large snowfall event accounted for 26% of the 1982 annual P and nearly half of all snow that fell that water year. While this snow was included in water year 1982, most energy-water transformations occurred in

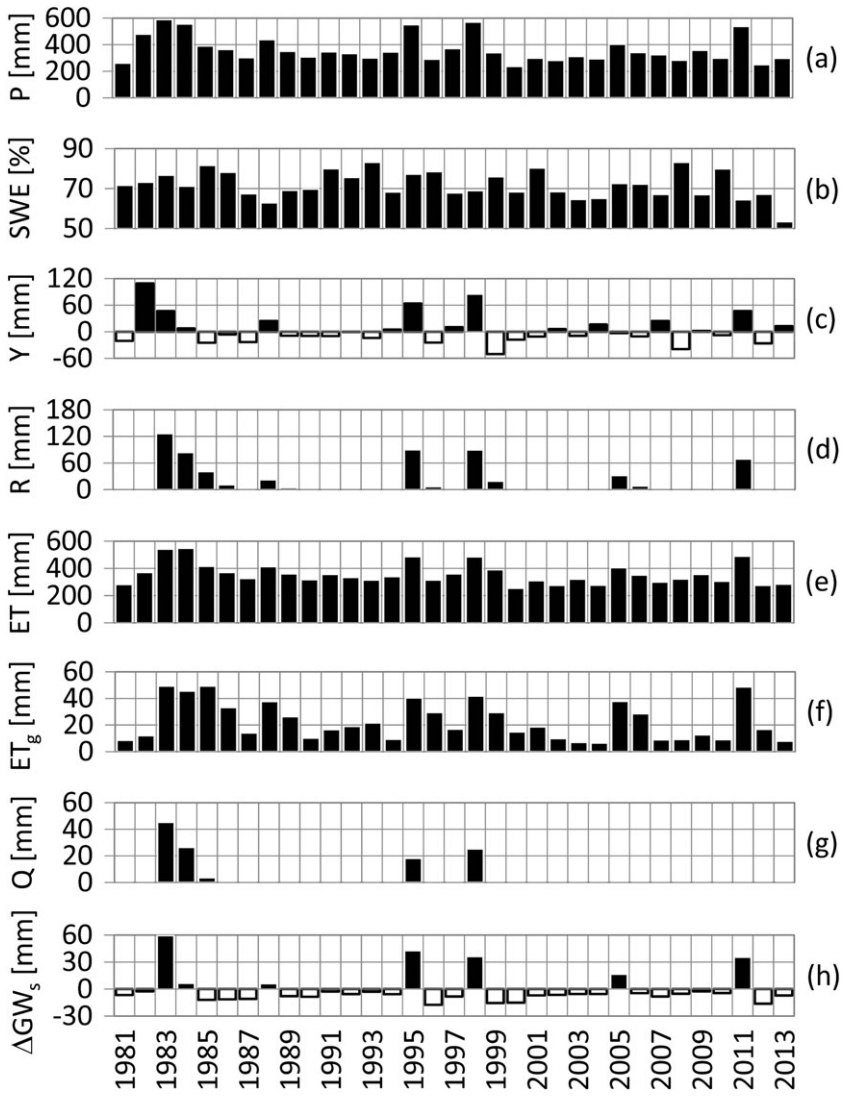

FIGURE 7 Baseline mean annual water budget components for (a) precipitation, (b) snow water equivalent as % of precipitation (c) yield, (d) recharge, (e) evapotranspiration, (f) groundwater ET, (g) stream discharge, and (h) change in groundwater storage. Yield is precipitation minus evapotranspiration (P-ET); negative values are shown in white

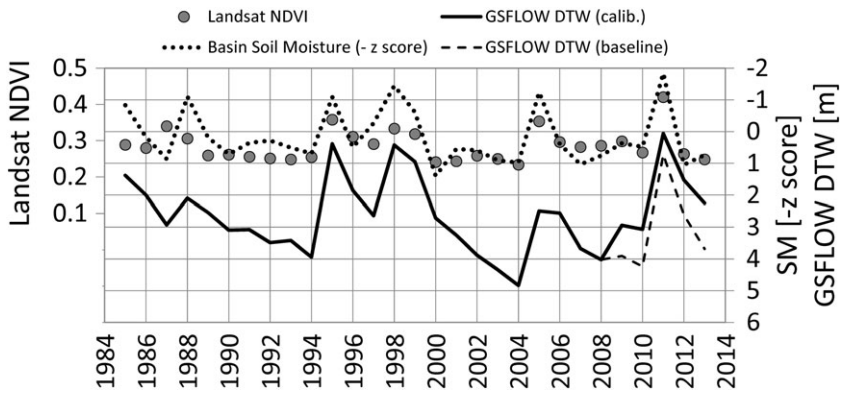

FIGURE 8 Comparison of Landsat-derived mean August normalized difference vegetation index (NDVI) for the meadow area and simulated values for soil moisture (SM, z score) and depth to water (DTW). Note that the z score is provided as a negative to plot on the same axis as DTW

October, or water year 1983, and could be considered part of the 1983 water budget along with the positive yield associated with this snowfall event. Subsequently, 1982 produces no recharge, no stream discharge, and experienced a decline in groundwater storage despite P > 400 mm/y and having P > ET. Overall, P surpassed the P threshold eight times, or approximately once every 4 years with an average yield of 9% (48 mm/y) during these wet years. Most years, P was less than 400 mm/y and the watershed operated in deficit (P-ET < 0). During dry years, vegetation must draw upon available soil moisture, thereby limiting recharge; or on shallow groundwater reserves from meadow and riparian complexes. Numerically, groundwater ET was simulated as a linear function based on an extinction depth. Water also can be used from the unsaturated zone if roots extend past the soil zone based on a wilting point threshold of water content. These processes are initiated only if water stored in the soil zone is not sufficient to meet ET demand based on vegetation type and density. Storage

depletion resulted in a lowering of water table elevations, failure of the stream to flow, and reduced groundwater flux to the alluvial fan. Relative fractions of simulated water budget components along with dynamics between budget components during wet and dry years were similar to previously published findings in watersheds in central and northern Nevada (Jeton et al., 2007; Huntington & Niswonger, 2012; Tang et al., 2016) with a conceptual model in which most, if not all, P is consumed annually, and deep rooted PJ and the meadow area increasing ET via access of deeper soil moisture, fractured bedrock reserves, and consumption of shallow groundwater.

6.3 | NDVI

We compared mean August meadow area NDVI to mean August simulated standardized soil moisture (z score) and mean August DTW within the meadow area as an independent evaluation of model performance (Figure 8). Baseline DTW also is shown to illustrate that with no PJ removal in 2009, average DTW was approximately 1 m deeper in the meadow than if 2009 PJ treatment occurred. Results show that simulated August soil moisture and DTW were highly correlated with NDVI, with $\rho = 0.77$ ($p < .01$) and $\rho = -0.71$ = ($p < .01$), respectively. An NDVI >0.3 corresponds to above average soil moisture (z score > 0). Simulated groundwater levels in the meadow showed a decline most years when soil moisture was at or below average conditions, indicating a water-limited system in which yield became negative as water was extracted from storage by deeper-rooted vegetation. Groundwater levels in the meadow only rebounded during wet years when enough P occurred to promote sufficient recharge and increased groundwater storage. While wet years only occurred intermittently, they were important in resetting DTW in the meadow and establishing a mean DTW of 2.5 m.

6.4 | Sensitivity to changes in PJ and temperature

Changes in mean annual water budget components from baseline given pre-expansion PJ conditions and mid-century temperature change are illustrated in Figure 9. The small-scale PJ scenario is not included since changes to water budget components were small and undistinguishable at the temporal and spatial scale of the figure. Given that changes in yield are defined as ΔP-ΔET and ΔP = 0, then all changes in yield are the result of simulated changes in ET. Changes in water partitioning were largest in years when $P > 400$ mm/y. Years in which $P \leq 400$ mm/y experienced only small changes in ET, and produced no change in stream discharge.

Reverting the watershed to pre-expansion conditions resulted in decreased ET and increased recharge, groundwater storage, and stream discharge. Overall, when $P > 400$ mm/y, changes in yield through changes in ET due to vegetation shifts were 20 ± 11 mm/y or 4 ± 2%, compared to baseline. For mid-century warming, results showed that more P fell as rain with an 80 mm/y reduction in SWE, an increase in ET, decrease in stream discharge and recharge, and a decrease in groundwater storage. Decreases in yield during wet years compared to baseline average were 15 ± 18 mm/y or 3 ± 3%. Large variability in response was based on air temperature of the baseline scenario. To illustrate, a comparison of water years 1998 and 2011

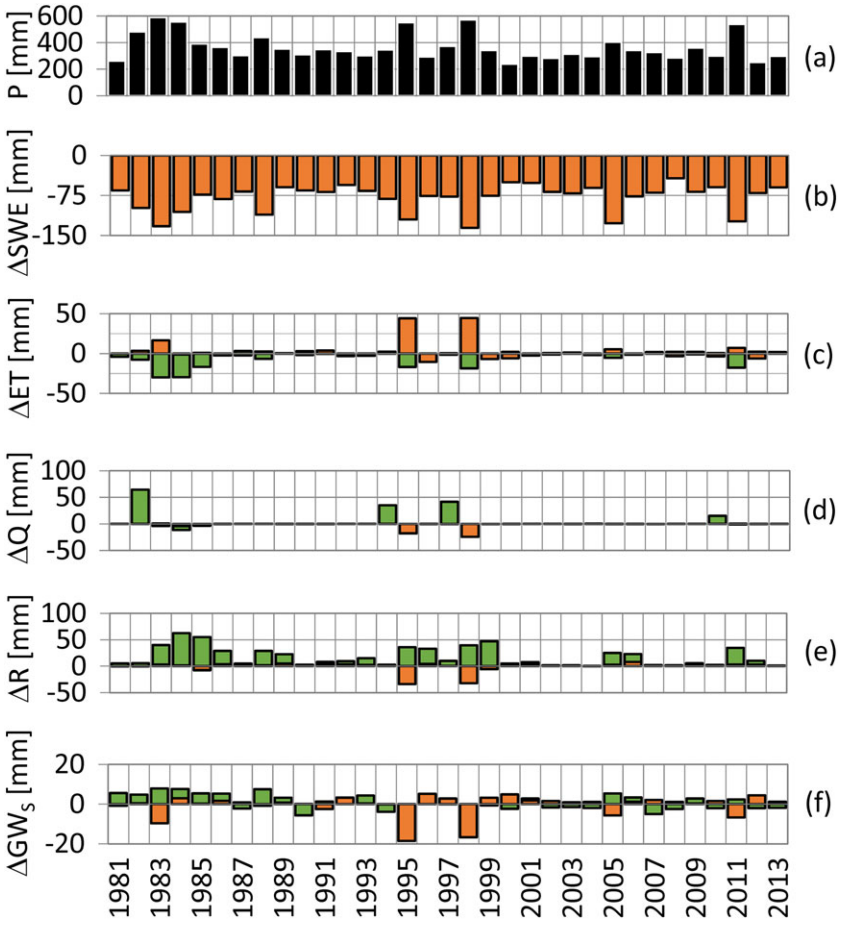

FIGURE 9 Watershed annual (a) precipitation; and changes from baseline for (b) SWE, (c) ET, (d) stream discharge, (e) recharge, and (g) groundwater storage. Pre-expansion Pinyon-Juniper (green); mid-century temperature (orange). Changes in pre-expansion SWE are negligible at this scale. Given that changes in yield equal ΔP-ΔET and ΔP = 0, then changes in yield are expressed as −ΔET

shows that 1998 changes in ET were much larger. Both years had nearly equal P, but Figure 7 indicates 2011 had significantly lower yield under baseline conditions. With no mid-century increase in temperature, 2011 was 1°C warmer than 1998, with October, December, and January more than 2°C warmer. More winter rain reduced SWE by 20% compared to 1998 and increased winter temperatures resulted in significant snowmelt in January and February which in turn reduced soil moisture in the spring, forcing greater reliance on groundwater sources to meet ET demand with the basin becoming water limited (ET/PET < 1) by early May. This dampened recharge fluxes and limited streamflow. In comparison, 1998 did not become water limited until late June. Increasing air temperature by an additional 3°C limited 2011 changes in ET because the system was already water limited during peak demand, while 1998 had ample soil moisture to accommodate increased PET in response to mid-century temperatures.

Changes in ET even for wet years were relatively small, with the watershed limiting water budget response through spatial and temporal redistribution of ET components. Figure 10 compares aggregated watershed response when P > 400 mm/y. Total ET was largely driven by soil evaporation and transpiration which were, in turn, controlled by PET. PET was low in the winter and began to rise sharply in May with rising air temperatures to peak in late July. A decline in simulated PET occurred in June based on increased probability of rain events during wet years during the course of this month and an associated decrease in simulated solar radiation. Similarly, monsoonal rains in late summer lowered PET below peak. ET through sublimation and canopy evaporation was expressed during the winter and spring while groundwater ET occurred in the late summer. These components were relatively small compared to soil ET when aggregated across the watershed. Under baseline conditions, the ratio of ET to PET showed the watershed was operating below potential much of the year as a result of reduced soil moisture. Soil moisture and recharge both increased with SWE depletion (snowmelt). Under assumed pre-expansion conditions, there were no large temporal swings in ET. The largest temporal changes in ET under pre-expansion conditions were primarily because of reduced groundwater ET in the late summer. These reductions did not produce large swings in ET. Instead, watershed-scale temporal changes were largely driven by changes in vegetation structure. Removing PJ and replacing with a mix of grass, shrubs, and bare ground decreased canopy closure and increased solar radiation transmission allowing greater melt in the spring when soil moisture was high, and ET was not limited. The timing of this additional water promoted significantly more recharge. In contrast to changing vegetation, increasing temperature promoted large seasonal shifts in all water budget components (Figure 10). As in pre-expansion conditions, soil ET was the dominant mechanism of total ET. Soil ET increased in the winter and early spring as a result of increased PET and increased soil moisture responding to more P falling as rain and faster snowmelt. Excess water in the winter was routed to recharge when the system was not water limited, producing a peak in recharge that was 2 months earlier than baseline at 60% of the maximum baseline rate. Soil ET rates dropped in May in response to less available snowmelt from a reduced snowpack

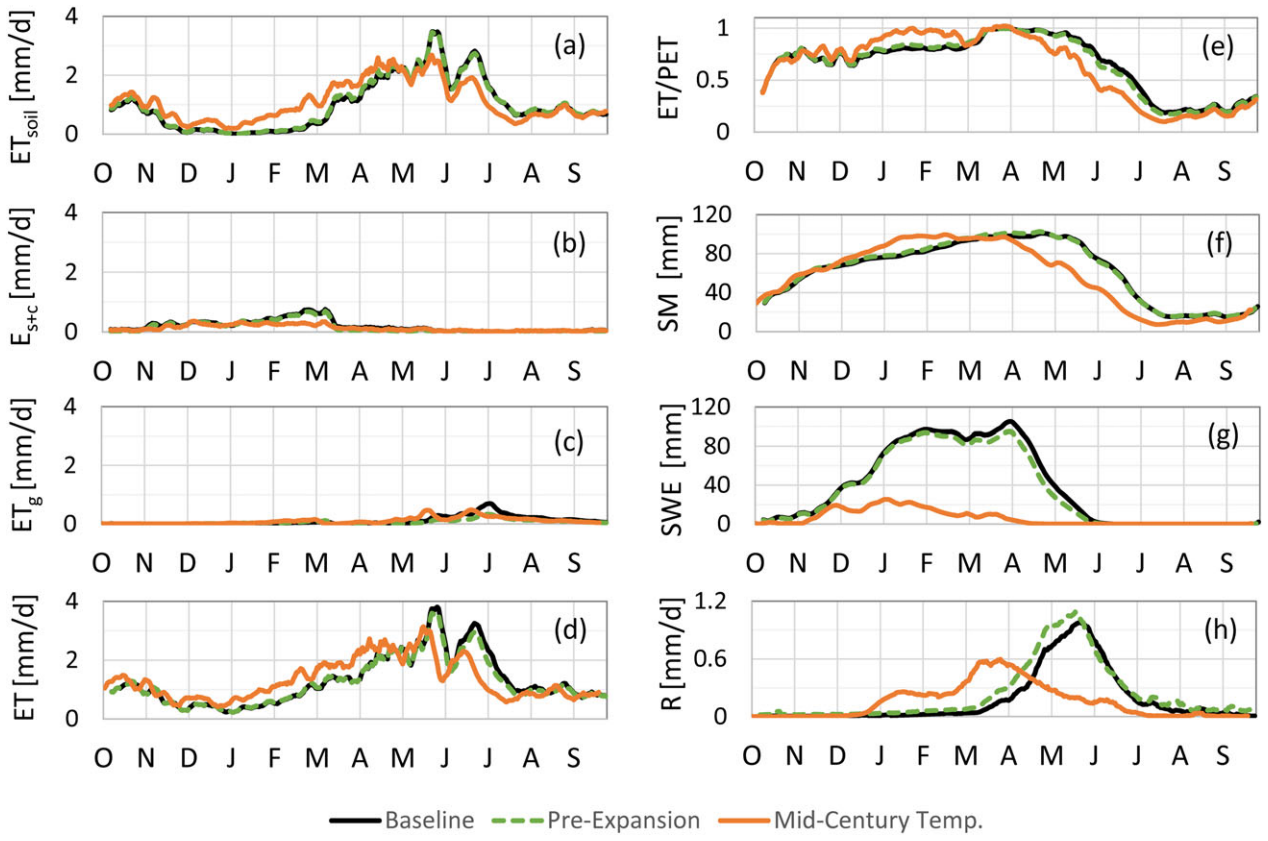

FIGURE 10 A comparison of several water budget components. Plots are watershed aggregated means for wet years (P > 400 mm/y) for (a) soil evaporation and transpiration, (b) sublimation and canopy evaporation, (c) groundwater evapotranspiration, (d) total ET, (e) the ratio of total ET to potential evapotranspiration, (f) soil moisture, (g) snow water equivalent (SWE), and (h) recharge. Plots are 7-day averages.

and rapid soil drying. Water limitations in soils forced ET < PET as early as April, and soil ET was lowered compared to baseline conditions. Groundwater ET compensated with slight increases above baseline in the spring but fell below baseline groundwater ET later in the summer in response to a falling water table. Subsequently, water limitations effectively reduced ET losses and modulated system response to temperature increases at the annual timescale.

Figure 11 illustrates the spatial distribution of baseline ET and mean annual change from baseline for the 8 years in which P > 400 mm/y. Baseline ET was highest in the alluvium where groundwater was closer to land surface, along hillslope toes where deep-rooted PJ had access to saturated groundwater and along aspects facing south and west where solar radiation and temperature adjustments increased PET. P was directly related to elevation and limited ET in the lower elevations of the watershed. Shifting basin vegetation away from PJ and toward a grass-shrub mix produced large spatial redistributions of ET. Specifically, hillslopes saw significantly decreased ET in both small-scale (Figure 11b) and pre-expansion PJ (Figure 11c) scenarios and increased ET in alluvial drainages in response to increased shallow water tables and increased groundwater ET. In contrast, climate warming (Figure 11d) displayed a more muted spatial response but promoted increased ET along most hillslopes, while some alluvial valleys experienced a decrease in ET as water table elevations declined and phreatophyte access to groundwater diminished. Northern aspects tended to have lower PJ canopy densities and contained more shrubs and therefore higher solar radiation transmission coefficients. Increasing temperature promoted faster soil drying and earlier onset of water limitation with the hydrologic simulation estimating reductions in ET along these hillslopes compared to baseline. In all scenarios, the greatest changes in ET occurred primarily along the edge of the hillslope adjacent to the alluvium. This region is a transition zone where saturated water levels were accessible to PJ and changes in ET were the combined effects of both ET from the soil zone and groundwater. With movement up the hillslope, the water table diverged from land surface and PJ were limited to water uptake in the unsaturated soil and weathered bedrock.

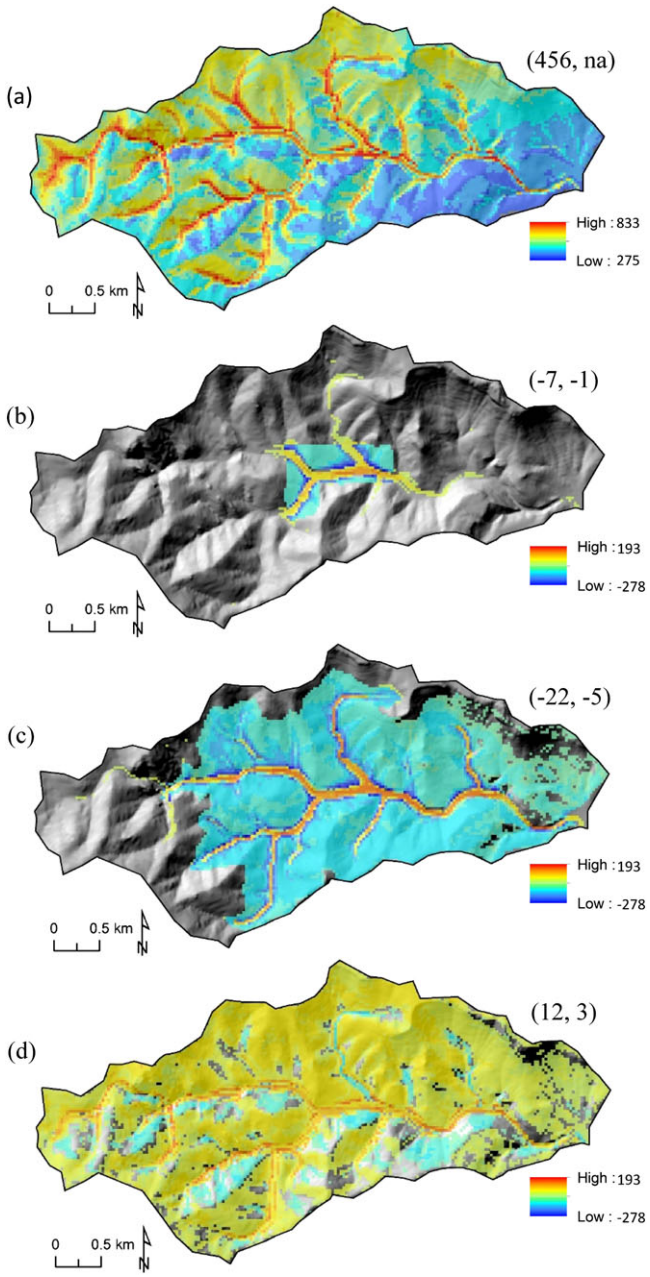

FIGURE 11 Aggregated mean for simulated spatial distribution of ET (mm/y) for a wet year (P > 400 mm/y): (a) baseline total evapotranspiration; and differences in ET from baseline given (b) small-scale PJ treatment, (c) pre-expansion conditions, and (d) mid-century temperature. Values <±5 mm/y masked out in (b–d). Basin mean (mm/y, % difference from baseline) provided

Lastly, Figure 12 shows predicted mountain meadow DTW for all scenarios tested. Results indicate that even small-scale changes in PJ produced significant changes in DTW beneath the meadow despite imperceptible changes in ET at the annual watershed scale. DTW is 1.0 m shallower compared to baseline. A return to pre-expansion PJ resulted in a 2 m decrease from baseline, or an average DTW = 0.5 m. Water levels were near land surface except during prolonged droughts in which DTW hovered at 1 m. In both cases, changes in PJ produced DTW with a greater resistance to water level declines during extended dry periods and reduced simulated intra-annual variability in response. Projected changes to mid-century temperature conditions resulted in a mean DTW of 3.2 m or 70 cm greater depth than baseline. The largest changes in DTW occurred during the wettest years when changes in ET were largest. As a consequence, the meadow DTW was unable to fully recover from drought conditions and the water table elevations in the meadow declined through time.

7 | DISCUSSION

Mountain meadows represent a subset of GDEs in the Great Basin that rely on shallow subsurface expressions of water to provide critical habitat for many sensitive species, such as the greater sage-grouse (*Centrocercus urophasianus*). Recent work has related functional type and vigor of vegetation in GDEs, as expressed with NDVI, correlated to DTW as a consequence of groundwater pumping (Huntington et al., 2016). Very little is understood about how mountain meadows will respond hydrologically to changes in upland vegetation or climate, and there is a need to develop effective adaptive management frameworks for these meadows and the ecosystems they support. The tight

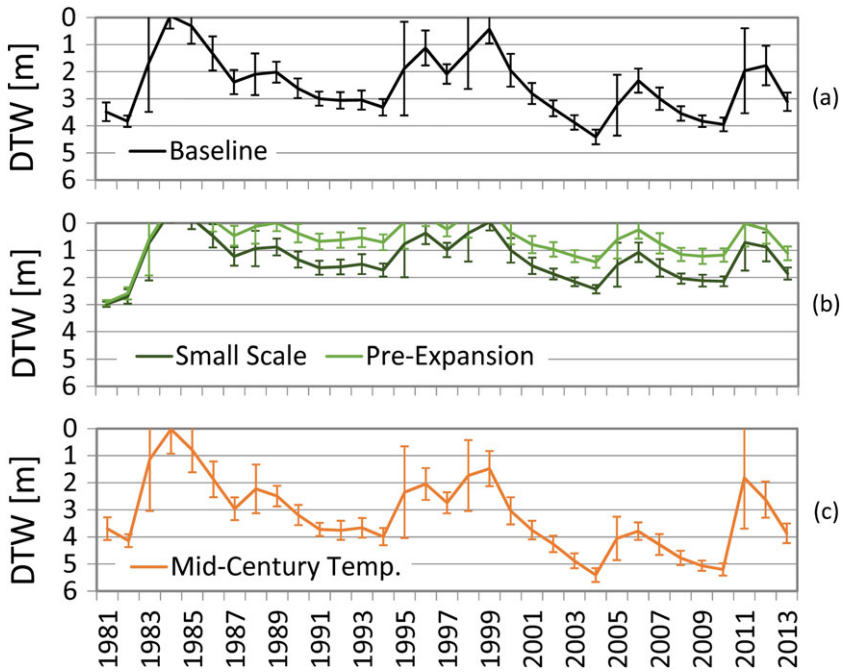

FIGURE 12 Average, annual depth to water (DTW) in the mountain meadow for (a) baseline, (b) changes in PJ, and (c) mid-century temperature. Error bars are predicted standard deviation for simulated monthly water levels for given water year

coupling of plant phenology with climatological and hydrological controls becomes critical in predictive understanding. Therefore, integrated hydrologic models are needed to allow for complex interplay between the atmosphere and land with inclusion of groundwater to capture the full suite of energy and water budget components important to these systems. GSFLOW allows these processes to be simulated and indicates that the PCEW operates on a threshold response to P. Years with $P \leq 400$ mm/y were water limited with ET consuming all P and drawing on stored soil moisture and groundwater. Consequently, water levels declined in the meadow. Years with $P > 400$ mm/y provided enough P to recharge groundwater and streams, although large variability in recharge could occur with warmer years resulting in more rain and less recharge. A similar P threshold has been reported by Hibbert (1983) who suggested that woodlands can only control streamflow if annual P is at least 460 mm/y, with this threshold lowered to 400 mm/y in snow dominated systems. This is the same order of magnitude suggested by Adams et al. (2012) of 500 mm/y for influencing yield in forests impacted by die-off. These comparisons imply a universal threshold in P, with water-limited conditions trumping the effects of vegetation and temperature.

Recently, developed cloud computing technology with Google EE has enhanced the ability to perform long time series assessment with Landsat satellite archives using images available at 30 m resolution from 1984 to present and with relatively high-temporal frequency at 16 days for Landsat 5 thematic mapper (1984 to 1999) and 8 days for Landsat 5, Landsat 7 enhanced thematic mapper (1999 to 2013), Landsat 7, and Landsat 8 OLI (2013 to present). Huntington et al. (2016) demonstrated the value of these data sets for studying GDEs in a variety of semiarid, land management contexts where there is significant temporal and spatial variability in vegetation vigor based on water availability. This work showed correlations between changes in vegetation vigor, as reflected in NDVI, as functions of P, evaporative demand, depth to groundwater, and groundwater pumping. We extended these ideas to evaluate GDE vigor in a mountain meadow setting to provide model evaluation similar to work by Carroll et al. (2015). In this manner, we linked an intensive numeric modeling platform to both shorter-term, ground-based observations and long-running Landsat data sets to span spatial and temporal scales of analysis. Calibrated model results were able to match observed solar radiation and ET_0 at the SCAN station located in the meadow and replicate observed groundwater levels across more than 100 m in elevational gradient. DTW estimates were in agreement with individual wells, although some predictive error occurred largely based on a mismatch between the virtual point measurement of the piezometer and the 30 m averaging of landscape and vegetation parameters to the GSFLOW grid. Significant correlation between NDVI and predicted soil moisture and DTW provided both means to corroborate the independently derived hydrologic state of the meadow as well as offer a mechanism for future evaluation of meadow systems across the landscape with emphasis on drought monitoring. PCEW indicated an NDVI threshold of 0.3 can distinguish between years of adequate soil moisture and shallow groundwater to support GDE vigor as well as those years when the system is in hydrologic decline with ecosystems becoming vulnerable. Future work will need to look at alternative timescales of drought, as well as the effect of type and duration of drought on ability of GDEs to rebound in their response. The combined use of integrated hydrologic models and remotely sensed data provides the ability to develop conceptual understanding of these systems and the potential precision needed to detect both short- and long- term changes in GDE vegetation vigor and resilience to declines in soil moisture and groundwater levels. The coupled approach builds a framework for improved monitoring and conservation of these systems.

Numerical models can provide predictive abilities beyond empirical relationships reliant on environmental gradients and offer a powerful tool to perform hypothetical, large-scale changes of landscape or climatic variables not practical to alter in ground-based observational experiments. Model results indicate that removing upland PJ produced

undetectable changes in watershed-scale annual yield estimates for small-scale removal projects similar to those conducted in 2009 at 0.5 km^2. Imperceptible gains with the small-scale treatment were in agreement with harvest literature suggesting a 20% reduction in forest cover is necessary to statistically detect a change in yield (Stednick, 1996; Brown, Zhang, McMahon, Western, & Vertessy, 2005). The muted response of ET to even large-scale alteration of upland vegetation suggested the system is not sensitive to PJ at the multi-decadal level and that even isolating wet years; changes in yield were limited to 20 mm/y (4%), which is significantly less than interannual variability in P. In terms of water budget partitioning, tree-scale measurements showed that a single juniper tree can consume nearly all available water, resulting in no deep percolation or runoff (Wilcox et al., 2006). The removal of a single tree would imply large changes in yield if done at the hillslope or watershed scale. These water savings do not scale up across the watershed, however, because the savings do not address canopy spacing or replacement vegetation nor repartitioning in ET across the watershed as a result of these changes. Livneh et al. (2015) simulated initial increases in yield as a result of tree mortality between 8 and 13%, but these yields were halved when understory vegetation developed. Dugas, Hicks, and Wright (1998) and Huang, Wilcox, Stern, and Perotto-Baldivieso (2006) reported stand and water yield increases based on juniper removal on the order 5 to 11%, while research related to altered energy and water budgets following large-scale tree mortality found limited effects on increased stream flow because greater soil evaporation and snowpack sublimation counteracted reductions in plant transpiration and canopy interception evaporation (Guardiola-Claramonte et al., 2011; Pugh & Small, 2012; Biederman et al., 2014).

The PCEW GSFLOW small-scale and pre-expansion scenarios accounted for replacement vegetation. Focusing on wet years, when change in yield is predicted to be largest, model results indicated little temporal variability in ET in comparison to baseline. The majority of water was consumed from the soil zone through evaporation and plant transpiration largely driven by PET process and moisture availability. While ET shifts in time were muted at the watershed scale, replacement vegetation was simulated to effectively reduce canopy densities, increasing the transmission of solar radiation and promoting slightly faster snowmelt at a time when the watershed was not water limited. Outcomes of altered canopy cover and shading on snowmelt are supported by observations in Molotch et al. (2009) and Harpold et al. (2014) as well as modeling by Mikkelson et al. (2013). The timing of this excess water promotes recharge, and lateral movement of water toward topographic lows to dramatically decrease meadow DTW. The model simulations suggested that dry years allow slight increases in recharge and DTW in the meadow that were stabilized even during extended drought. While watershed scale ET shifts in time appeared small, the removal of PJ produced large spatial shifts in ET. Specifically, replacing PJ vegetation with a mix of shrubs, grass, and bare soils effectively reduced soil water uptake in the upland portions of the basin, as well as groundwater uptake by PJ along hillslope toes, with significant increases in transpiration loss along riparian and meadow complexes as DTW decreased in these regions. Redistribution occurred at the hillslope scale allowing even small-scale removal of PJ proximal to the meadow to significantly control meadow DTW and provide greater access to shallow groundwater for meadow vegetation. Preliminary work on stand transpiration in PCEW found that of 130 trees investigated, 64% were isohydric Pinyon and able to capitalize on wet conditions by increasing transpiration significantly when water availability increased. Isohydric behavior was not explicitly modeled by GSFLOW, and, as a consequence, it is likely the model under predicts ET savings with PJ removal. Nonetheless, the shift in hydrologic partitioning toward greater groundwater storage, decreased DTW in the alluvial sediments, and subsequent transpiration loss in the meadow, as opposed to consumption by PJ along the hillslopes, was simulated and likely has important ramifications on management of these GDEs.

Simulating increased temperatures to projected mid-21st century levels, with no change in P, produced little change at the multi-decadal scale of watershed hydrologic budgets. Instead, increases in ET as a function of increased temperature were isolated to years when $P > 400$ mm/y. Only during wet years, when the system was less water limited, can this change manifest itself. Even during these wet years, however, increased ET was relatively small at approximately 5%. In contrast to vegetation change, temperature increase promoted large seasonal swings based on increased PET and a shifting temporal pattern in soil moisture availability. An increased proportion of winter P falling as rain combined with faster snowmelt of a diminished snowpack increased soil storage in the winter and ET/PET approached 1.0 with excess water routed toward recharge. Peak recharge was shifted 2 months earlier and at a 60% reduction compared to baseline. Water limitation in the soil zone began as early as April to limit ET during the remainder of the year and offset the large increases in ET during the winter and early spring dampening changes in annual estimates of yield reduction. Spatially, increasing temperatures and associated atmospheric demand produced higher ET consumption across the watershed with the largest increases occurring along hillslope toes where PJ has access to groundwater. North facing slopes with lower canopy densities, however, showed a net reduction in ET related to increased transmission and earlier onset of water limitation; while some alluvial valleys showed a net decrease in ET as a result of increased DTW and reduced transpiration from groundwater. While temporal and spatial distributions of ET increases were mitigated by water limitation, the influence of reduced recharge was to limit rebound in meadow DTW during wet conditions and likely force the meadow toward dry and degraded meadow community structures.

Our results indicated that removing most PJ in the basin would not produce a perennial stream given climatic conditions of 1981–2013. Instead, anecdotal evidence suggesting consistent stream flow at the beginning of the 20th century was more likely related to wetter and cooler climatic conditions than to changes in upland PJ. A period of persistent and widespread wet conditions in the western U.S. (Arizona, California, Colorado, Idaho, Montana, Nevada, New Mexico, Utah, and Wyoming) from 1905 to1917 is noted in several studies (Fey, Stahle, & Cook, 2003; Webb, McCabe, Hereford, & Wilkowske, 2004; Woodhouse et al., 2005) with short duration but extreme P events occurring in high frequency. These studies used paleoclimate reconstruction of tree-ring data in combination with National Weather Service climate station networks to construct Palmer Drought Severity Index of P anomalies. Wetter conditions during this nine year period

were attributed to predominantly greater winter P and anomalously cool temperatures that slowed snowmelt and reduced evaporation (Woodhouse et al, 2005). Review of the temperature, P, and Palmer Drought Hydrologic Index specific to Nevada from 1895 to 2015 (NOAA, 2016) and several long-running discharge records in the state reveal that while the early 20th century pluvial period of wetter and cooler conditions produced above average streamflow; the period from 1969 to 1986 appeared the longest and wettest period in the state with 1983 generating the highest recorded discharge at many locations. Our model captures the very end of this extensive pluvial period and simulated both stream discharge and a significant rebound in the meadow's groundwater levels in response to these climatic drivers. Since the mid-1980s, the 10-year moving average for temperature and P indicated Nevada's climate experienced significant warming compared to the previous decades in the 20th century and a step-wise decrease in annual P. Evidence that wet and cool pluvial periods occurred prior to 1986, while warm and increasingly dry conditions have subsequently existed; corroborated with model results suggesting the influence of both P thresholds and the importance of temperature on P type and recharge timing and quantity, it is reasonable to suggest ephemeral stream conditions in PCEW in the late 20th century and early 21st century were primarily climatologically driven and not dictated by PJ expansion alone. The question still remains – which is more important to streamflow generation: wetter conditions or cooler temperatures? Our results suggested that the system is hydrologically controlled by P, with temperature modifying this response but only for those years in which the system is not water limited. The simulated period of 1981 to 2000 represented P of similar order to the early 20th century, but with temperatures approximately 0.5°C warmer and streamflow isolated to only those years with $P > 400$ mm/y. Hypothetically, it may be possible that cooler temperatures, more reflective of the early 20st century, could lower the P threshold and force the stream toward perennial conditions not simulated in the late 20th and early 21st century, but these experiments have not been run.

8 | CONCLUSIONS

The combination of GSFLOW simulations, ground-based observations, NDVI, and gridded climate products used in this study has proven useful for clarifying the causality of changing meadow conditions in PCEW; a semiarid, snow-dominated watershed in the Great Basin. Our research evaluated potential temperature and PJ controls on shallow groundwater response in a mountain meadow. Hydrologic conceptualization was based on the vegetation-streamflow framework in which woody-plants can access water at depths greater than non-woody plants. Additionally, we assumed that weathered and fractured bedrock has the ability to store water for PJ transpiration needs during water-limited periods in upland portions of the basin where soils are thin. Use of EE Landsat satellite and gridded climate archives afforded an independent measure of soil moisture that agreed well with model results and correlated significantly to simulated DTW in the meadow. Use of Landsat derived NDVI offerred a means to monitor GDEs and the potential to scale results across the landscape for drought monitoring efforts. Model simulations across three decades (1981–2013) indicated that the system was generally water limited with ET exceeding P to force depletion of storage such that meadow water levels declined in response to reduced recharge and vegetation using shallow groundwater reserves for consumptive needs. There was a threshold response in hydrology, however, to $P > 400$ mm/y. Only during these intermittent wet years did P exceed ET by 9% to promote streamflow and allow meadow groundwater levels to rebound to maintain a mean DTW of 2.5 m.

Integrated model results suggested water yield sensitivity to PJ or temperature increase was reserved for only these wet, intermittent years when there was enough water to impart change, with changes in yield kept small at approximately ±4% above baseline conditions. Reinstating the basin to assumed pre-expansion PJ growth did not produce a perennial stream. Anecdotal evidence of continuous streamflow in the early 20th century was more likely related to pluvial conditions widespread at that time and not to upland vegetation in the watershed. Muted response in yield was caused by spatial and temporal redistribution of ET. Specifically, removing PJ transferred ET consumption along the hillslopes to downgradient valleys where decreased DTW provided meadow vegetation access to groundwater sources; while increased temperatures resulted in large increases in winter soil ET that were offset by water limited conditions the remainder of the year. While changes in yield were small, vegetation structure combined with climate influenced the magnitude and timing of snowmelt with significant implications for recharge as a function of soil moisture conditions and PET. This had ecological ramifications in the receiving meadow via changes in DTW and stability in these water levels. DTW was estimated to decrease from 2.5 m under baseline conditions to 0.3 m for pre-expansion of PJ growth and was capable of supporting a mostly wet, obligate phreatophytic community of Nebraska Sedge, which relied on a relatively shallow and stable groundwater system. Small-scale changes in PJ proximal to the meadow were simulated to decrease DTW in the meadow by 1 m from baseline conditions with reduced variability in DTW. Decreases in DTW with small-scale PJ removal could promote a more sustainable ecologic system potentially containing mostly wet and mesic phreatophytes. In contrast, modest temperature increases shifted the timing and reduced the magnitude of recharge in response to increased PET. The outcome was to limit DTW rebound in wet years. Mean meadow DTW increased by 70 cm compared to baseline to potentially destabilize ecosystem function in the meadow.

ACKNOWLEDGMENTS

Funding for this study was provided by the U.S. Bureau of Land Management grant #L13 AC00169, the U.S. Department of Agriculture Agricultural Research Service grant #59-5370-3-001 through the Great Basin Landscape Conservation Cooperative; Desert Research Institute Maki Endowment; U.S. Geological Survey 2012–2017 Landsat Science Team grant, and a Google Earth Engine faculty research grant.

REFERENCES

Abatzoglou, J. T., Hegewisch, K., Carroll, R. W., Lutz, A., Leising, J. F., Rajagopal, S., … Thomas, J. M. (2014). Impacts of a changing climate

on water resources in the eastern Great Basin. *Desert Research Report*, 41266416.

Adams, H. D., Luce, C. H., Vreshears, D. D., Allen, C. D., Weiler, M., Hale, V. C., … Huxman, T. E. (2012). Ecohydrological consequences of drought- and infestation triggered tree die-off: Insights and hypotheses. *Ecohydrology*, *5*, 145–159.

ASCE-EWRI. (2005). The ASCE standardized reference evapotranspiration equation, Report 0–7844-0805-X, ASCE Task Committee on Standardization of Reference Evapotranspiration, Reston, Virginia., American Society of Civil Engineers. Available at http://www. kimberly.uidaho.edu/water/asceewri/ Accessed June 14, 2014.

Baghzouz, M., Devitt, D. A., Fenstermaker, L. F., & Young, M. H. (2010). Monitoring vegetation phenological cycles in two different semi-arid environmental settings using a ground-based NDVI system: A potential approach to improve satellite data interpretation. *Remote Sensing*, *2*(4), 990–1013.

Beamer, J. P., Huntington, J. L., Morton, C. G., & Pohll, G. M. (2013). Estimation of annual groundwater evapotranspiration from phreatophyte vegetation in the Great Basin using Landsat EVI and flux tower measurements. *Journal of the American Water Resources Association*, *49*(3), 518–533.

Bearup, L. A., Maxwell, R. M., Clow, D. W., & McCray, J. E. (2014). Hydrological effects of forest transpiration loss in bark beetle-impacted watersheds. *Nature Climate Change*, *4*(6), 481–486. DOI: 10.1038/nclimate2198

Belcher, W. R., Elliot, P. E., Geldon, A. L. (2001). Hydraulic-property estimates for use with a transient ground-water flow model of the Death Valley regional ground-water flow system, Nevada and California: U.S. Geological Survey Water-Resources Investigations Report 01–4210 (p. 28).

Biederman, J. A., Harpold, A. A., Gochis, D. J., Ewers, B. E., Reed, D. E., Papuga, S. A., & Brooks, P. D. (2014). Increased evaporation following widespread tree mortality limits streamflow response. *Water Resources Research*, *50*, 5395–5409. DOI:10.1002/2013WR014994.

Brooks, M. L., D'Antonio, C. M., Richardson, D. M., Grace, J. B., Keeley, J. E., DiTomaso, J. M., … Pyke, D. (2004). Effects of invasive alien plants on fire regimes. *Bioscience*, *54*, 677–688.

Brown, A. E., Zhang, L., McMahon, T. A., Western, A. W., & Vertessy, R. A. (2005). A review of paired catchment studies for determining changes in water yield resulting from alterations in vegetation. *Journal of Hydrology*, *310*, 28–61.

Carroll, R. W. H., Pohll, G. M., Morton, C. G., & Huntington, J. L. (2015). Calibrating a basin-scale groundwater model to remotely sensed estimates of groundwater evapotranspiration. *Journal of American Water Resources Association*, *51*(4), 1114–1127.

Chambers, J. C. (2008). Climate change in the Great Basin. USDA Forest Service General Technical Rep. RMRS-GTR-204 (p. 4).

Chambers, J. C., Miller, R. F., Board, D. I., Grace, J. B., Pyke, D. A., Roundy, B. A., … Tausch, R. J. (2014). Resilience and resistance of sagebrush ecosystems to management treatments: Implications for state and transition models. *Rangeland Ecology and Management*, *67*(5), 440–454.

Daly, C., Neilson, R. P., & Phillips, D. L. (1994). A statistical-topographic model for mapping climatological precipitation over mountainous terrain. *J. Applied Meteorology*, *33*, 140–158.

Devitt, D. A., Fenstermaker, L. F., Young, M. H., Conrad, B., Baghzouz, M., & Bird, B. M. (2011). Evapotranspiration of mixed shrub communities in phreatophytic zones of the Great Basin region of Nevada (USA). *Ecohydrology*, *4*(6), 807–822.

Dugas, W. A., Hicks, R. A., & Wright, P. (1998). Effect of removal of *Juniperus ashei* on evapotranspiration and runoff in the Seco Creek watershed. *Water Resources Research*, *34*, 1499–1506.

Fey, F. K., Stahle, D. W., & Cook, E. R. (2003). Paleoclimatic analogs to 20th century moisture regimes across the United States. *Bulletin of American Meteorological Society*, *84*, 901–909.

Fritts, H. C. (1974). Relationships of ring widths in arid site conifers to variations in monthly temperature and precipitation. *Ecological Monographs*, *44*, 411–440.

Fritts, H. C., & Wu, X. (1986). A comparison between response function analysis and other regression techniques. *Tree-ring Bulletin*, *46*, 31–46.

Grover, H. D., & Musick, H. B. (1990). Shrubland encroachment in southern New Mexico, U.S.A: An analysis of desertification processes in the American southwest. *Climate Change*, *17*, 305–330.

Guardiola-Claramonte, M., Troch, P. A., Breshears, D. D., Huxman, T. E., Switanek, M. B., Durcik, M., & Cobb, N. S. (2011). Decreased streamflow in semi-arid basins following drought-induced tree die-off: A counter-intuitive and indirect climate impact on hydrology. *Journal of Hydrology*, *406*, 225–233.

Harbaugh, A. W. (2005). MODFLOW-2005, the U.S. Geological Survey modular groundwater model—the ground-water flow process, U.S. Geol. Survey Technical Methods, Book 6, Chap. A16.

Harpold, A. A., Biederman, J. A., Condon, K., Merino, M., Korgaonkar, Y., Nan, T., … Brooks, P. D. (2014). Changes in snow accumulation and ablation following the Las Conchas forest fire, New Mexico. *USA. Ecohydrology*, *7*, 440–452. DOI: 10.1002/eco.1363

Hibbert, A. R. (1983). Water yield improvement potential by vegetation management on western rangelands. *Water Resources Bulletin*, *19*, 375–381.

Huang, Y., Wilcox, B. P., Stern, L., & Perotto-Baldivieso, H. (2006). Springs on rangelands: Influence of woody plant cover and runoff dynamics. Hydrological. *Processes*, *20*(15), 3277–3288.

Huntington, J. L., & Niswonger, R. G. (2012). Role of surface-water and groundwater interactions on projected summertime streamflow in a snow dominated region: An integrated modeling approach. *Water Resources Research*, *48*(11). DOI: 10.1029/2012WR012319

Huntington, J. L., Niswonger, R. G., Rajagopal, S., Zhang, Y., Gardner, M., Morton, C., Reeves, D. M., McGraw, D., Pohll, G. M. (2013). Integrated hydrologic modeling of Lake Tahoe and Martis Valley Mountain Block and Alluvial Systems, Nevada and California. Proceedings Paper, MODFLOW and More 2013, June 2–5, 2013, Golden, Colorado.

Huntington, J., McGwire, K., Morton, C., Snyder, K., Perterson, S., Ericson, T., Niswonger, R., Carroll, R. W. H., Smith, G. (2016). Assessing the role of climate and resource management on groundwater dependent ecosystem changes in arid environments with the Landsat archive. *Remote sensing of Environment*. DOI: 10.1016/j.rse.2016.07.004

Huxman, T. E., Wilcox, B. P., Breshears, D. D., Scot, R. L., Snyder, K. A., Small, E. E., … Jackman, R. B. (2005). Ecohydrological implications of woody plant encroachment. *Ecology*, *86*, 308–319.

LANDFIRE. (2008). Existing vegetation type layer, LANDFIRE 1.1.0, U.S. Department of the Interior, Geological Survey. Retrieved from: http://landfire.cr.usgs.gov/viewer/ (Accessed 13 September 2013)

Leavesley, G. H., Markstrom, S. L., Viger, R. J., & Hay, L. E. (2005). USGS modular modeling system (MMS) — precipitation-runoff modeling system (PRMS) MMS-PRMS. In V. Singh, & D. Frevert (Eds.), *Watershed Models: Boca Raton* (pp. 159–177). Fla.: CRC Press.

Livneh, B., Deems, J. S., Buma, B., Barsugli, J. J., Schneider, D., Molotch, N. P., … Wessman, C. A. (2015). Catchment response to bark beetle outbreak and dust-on-snow in the Colorado Rocky Mountains. *Journal of Hydrology*, *523*, 196–210.

Madsen, M. D., Petersen, S. L., Neville, K. J., Roundy, B. A., Taylor, A. G., & Hopkins, B. G. (2012). Influence of soil water repellency on seedling emergence and plant survival in a burned semi-arid woodland. *Arid Land Research and Management*, *26*, 236–249. DOI:10.1080/15324982.2012.680655.

Mallick, K., Bhattacharya, B. K., & Patel, N. K. (2009). Estimating volumetric surface moisture content for cropped soils using a soil wetness index based on surface temperature and NDVI. *Agricultural and Forest Meteorology*, *149*(8), 1327–1342.

Markstrom, S. L., Niswonger, R. G., Regan, R. S., Prudic, D. E., Barlow, P. M. (2008). gsflow-coupled ground-water and surface-water flow model based on the integration of the precipitation-runoff modeling system

(prms) and the modular ground-water flow model (MODFLOW-2005): U.S. Geological Survey Techniques and Methods 6-D1, 240 p.

McGwire, K., Minor, T., & Fenstermaker, L. (1999). Hyperspectral mixture modeling for quantifying sparse vegetation cover in arid environments. *Remote Sensing of Environment*, *72*, 360–374.

Mikkelson, K. M., Maxwell, R. M., Ferguson, I., Stednick, J. D., McCray, J. E., & Sharp, J. O. (2013). Mountain pine beetle infestation impacts: Modeling water and energy budgets at the hill-slope scale. *Ecohydrology*, *6*, 64–72. DOI: 10.1002/eco.278

Miller, R. F., & Rose, J. A. (1999). Fire history and western juniper encroachment in sagebrush steppe. *Journal of Range Management*, *52*, 550–559.

Miller, R. F., Svejcar, T. J., & Rose, J. A. (2000). Impacts of western juniper on plant community composition and structure. *Journal of Rangeland Management*, *53*, 574–585.

Miller, R. F., Bates, J. D., Svejcar, T. J., Pierson, F. B., Eddleman, L. E. (2005). Biology, ecology and management of western Juniper (*Juniperus occidentalis*). Technical Bulletin 152. Oregon State University, Agricultural Experiment Station (p. 82).

Miller, R. F., Tausch, R. J., McArthur, E. D., Johnson, D. D., Sanderson, S. C. (2008). Age structure and expansion of pinon-juniper woodlands: A regional perspective in the Intermountain West. Res Pap RMRS-RP-69. For Collins, CO: US Department of Agriculture, Forest Service, Rocky Mountain Research Station (p. 15).

Mitchell, K. E., Lohmann, D., Houser, P. R., Wood, E. F., Schaake, J. C., Robock, A., & Bailey, A. A. (2004). The multi-institution North American Land Data Assimilation System (NLDAS): Utilizing multiple GCIP products and partners in a continental distributed hydrological modeling system. *Journal of Geophysical Research: Atmospheres (1984–2012)*, *109*(D7).

Mollnau, C., Newton, M., & Stringham, T. (2014). Soil water dynamics and water use in a western Juniper (*Juniperus occidentalis*) woodland. *Journal of Arid Environments*, *102*, 117–126.

Molotch, N. P., Brooks, P. D., Burns, S. P., Litvak, M., Monson, R. K., McConnell, J. R., & Musselman, K. (2009). Ecohydrological controls on snowmelt partitioning in mixed-conifer sub—alpine forests. *Ecohydrology*, *2*, 129–142. DOI:10.1002/eco.48.

Moore, R. T., Hansen, M. C. (2011). Google Earth Engine: A new cloud-computing platform for global-scale earth observation data and analysis. AGU Fall Meeting Abstracts. 1: p. 02.

Mote, P. W., Hamlet, A. F., Clark, M. P., & Lettenmaier, D. P. (2005). Declining mountain snowpack in western North America. *Bulletin of the American Meteorological Society*, *86*, 39–49.

Natural Resources Conservation Service. (1991). United States Department of Agriculture. Web Soil Survey. Retrieved from: http://websoilsurvey.nrcs.usda.gov/ Accessed November, 2013.

Nichols, W. D. (2000). Regional groundwater evapotranspiration and groundwater budgets, Great Basin, Nevada. U.S. Geological Survey Professional Paper 1628 (p. 82).

Niswonger, R. G., Prudic, D. E. (2005). Documentation of the streamflow-routing (SFR2) package to include unsaturated flow beneath streams – a modification to the SFR1, US Geological Survey Technical Methods. 6-A13 (p. 51).

Niswonger, R. G., Panday, S., Ibaraki, M. (2011). MODFLOW-NWT, a newton formulation for MODFLOW-2005. Groundwater Resources Program. Techniques and Methods 6-A37 (p. 44).

NOAA. (2016). National Centers for Environmental Information, Climate at a Glance: U.S. Time Series. Published August 2016, retrieved on August 17, 2016 from http://www.ncdc.noaa.gov/cag/

PRISM Climate Group. (2015). *Oregon State University; 30-Year Normals.*, Retrieved from: http://prism.oregonstate.edu/normals/, downloaded November 5, 2015.

Pugh, E. T., & Gordon, E. S. (2013). A conceptual model of water yield effects from beetle induced tree death in snow-dominated lodgepole pine forests. *Hydrological Processes*, *27*, 2048–2060. DOI: 10.1002/hyp.9312

Pugh, E., & Small, E. (2012). The impact of pine beetle infestation on snow accumulation and melt in the headwaters of the Colorado River. *Ecohydrology*. DOI: 10.1002/eco.239

Qi, J., Chehbouni, A., Huete, A. R., Kerr, Y. H., & Sorooshian, S. (1994). A modified soil adjusted vegetation index. *Remote Sensing of Environment*, *48*(2), 119–126. DOI: 10.1016/0034-4257(94)90134-1

Rajagopal, S., Huntington, J. L., Niswonger, R., Pohll, G., Gardner, M., Morton, C., Zhang, Y., Reeves, D. M. (2015). Integrated Surface and Groundwater Modeling of Martis Valley, California, for Assessment of Potential Climate Change Impacts on Basin-Scale Water Resources. Desert Research Institute Publication No. 41261, prepared for U.S. Bureau of Reclamation (p. 54).

Regan, R. S., Niswonger, R. G., Markstrom, S. L., Barlow, P. M. (2015). Documentation of a restart option for the U.S. Geological Survey coupled groundwater and surface-water flow (GSFLOW) model: U.S. Geological Survey Techniques and Methods, book 6, chap. D3, 19 p., doi: 10.3133/tm6D3

Robles, M. D., Marshall, R. M., O′ Donnell, R., Smith, E. B., Haney, J. A., & Gori, D. F. (2014). Effects of climate variability on watershed-scale runoff in southwestern USA Ponderosa Pine forests. *PLoS ONE*, *9*(10) e111092. DOI: 10.1371/journal.pone.0111092

Ryel, R. J., Ivans, C. Y., Peek, M. S., & Leffler, A. J. (2008). Functional differences in soil water pools: A new perspective on plant water use in water-limited ecosystems. *Progress in Botany*, *69*, 397–422.

Ryel, R. J., Leffler, A. J., Ivans, C., Peek, M. S., & Caldwell, M. M. (2010). Functional differences in water-use patterns of contrasting life forms in Great Basin steppelands. *Vadose Zone Journal*, *9*, 548–560.

Salve, R., Rempe, D. M., & Dietrich, W. E. (2012). Rain, rock moisture dynamics, and the rapid response of perched groundwater in weathered, fractured argillite underlying a steep hillslope. *Water Resources Research*, *48*. DOI: 10.1029/2012WR012583.W11528

Schwinning, S. (2010). The ecohydrology of roots in rocks. *Ecohydrology*, *3*, 238–245. DOI: 10.1002/eco.134

Seibert, J., McDonnell, J. J., & Woodsmith, R. D. (2010). Effects of wildfire on catchment runoff response: A modelling approach to detect changes in snow-dominated forested catchments. *Hydrology Research*, *41*(5), 378–390.

Smith, J. L., Laczniak, R. J., Moreo, M. T., Welborn, T. L. (2007). Mapping evapotranspiration units in the Basin and Range Carbonate-Rock Aquifer System, White Pine County, Nevada, and adjacent areas in Nevada and Utah. U.S. Geological Survey Scientific Investigations Report 2007–5087, 31. Retrieved from: http://pubs. usgs.gov/sir/2007/5087/

Stednick, J. D. (1996). Monitoring the effects of timber harvest on annual water yield. *Journal of Hydrology*, *176*, 79–95.

Tang, G., Carroll, R. W. H., Lutz, A., & Sun, L. (2016). Regulation of precipitation-associated vegetation dynamics on catchment water balance in a semiarid and arid mountainous watershed. *Ecohydrology*. DOI: 10.1002/eco.1723

Tasumi, M., Allen, R. G., & Trezza, R. (2008). At-surface reflectance and albedo from satellite for operational calculation of land surface energy balance. *Journal of hydrologic engineering*, *13*(2), 51–63.

Tausch, R. J., Miller, R. F., Roundy, B. A., Chambers, J. C. (2009). Piñon and juniper field guide: Asking the right questions to select appropriate management actions: U.S. Geological Survey Circular 1335, 96.

Tucker, C. J. (1979). Red and photographic infrared linear combinations for monitoring vegetation. *Remote Sensing of Environment*, *8*(2), 127–150.

Wagner, F. H. (Ed) (2003). *Preparing for a changing climate – the potential consequences of climate variability and change. Rocky Mountain/Great Basin regional climate-change assessment team for the U.S. Global Change Research Program* (pp. 240). Logan, UT: Utah State University.

Walter, H. (1971). Natural savannahs as a transition to the arid zone. In: Oliver and Boyd (ed) *Ecology of tropical and subtropical vegetation*. Oliver and Boyd, Edinburgh, pp 238–265

Webb, R. H., McCabe, G. J., Hereford, R., Wilkowske, C. (2004). Climate fluctuations, drought and flow in the Colorado River Basin. U.S. Geological Survey Fact Sheet. 3062–04. US Department of the Interior. Lakewood, CO.

Welch, A. H., Bright, D. J., Knochenmus, L. A. (eds). (2007). Water resources of the Basin and Range carbonate-rock aquifer system, White Pine County, Nevada, and adjacent areas in Nevada and Utah: U.S. Geological Survey Scientific Investigations Report 2007–5261, 96.

Wilcox, B. P., Owens, M. K., Dugas, W. A., Ueckert, D. N., & Hart, C. R. (2006). Shrubs, streamflow, and the paradox of scale. *Hydrological Processes*, *20*, 3245–3259. DOI: 10.1002/hyp.6330

Woodhouse, C. A., Kunkel, K. E., Easterling, D. R., & Cook, E. R. (2005). The twentieth-century pluvial in the western United States. *Geophysical Research Letters*, *32*, L07701. DOI: 10.1029/2005GL022413

Wu, W. (2014). The generalized difference vegetation index (GDVI) for dryland characterization. *Remote Sensing*, *2014*(6), 1211–1233.

Zhang, L., Dawes, W. R., & Walker, G. R. (2001). Response of mean annual evapotranspiration to vegetation changes at catchment scale. *Water Resources Research*, *37*(3), 701–708.

Ziska, L. H., Reeves, J. B. III, & Blank, B. (2005). The impact of recent increases on CO2 on biomass production and vegetative retention of cheatgrass (*Bromus tectorum*): Implications for fire disturbance. *Global Change Biology*, *11*, 1325–1332.

How to cite this article: Carroll, RWH., Huntington, JL., Snyder, KA., Niswonger, RG., Morton, C., Stringham, TK. Evaluating mountain meadow groundwater response to Pinyon-Juniper and temperature in a great basin watershed. *Ecohydrol*. 2017;10:e1792. doi:10.1002/eco.1792.